AMERICAN SOCIETY FOR MICROBIOLOGY | Journal of Virology®

VIRUS-CELL INTERACTIONS

HIV Infection Stabilizes Macrophage-T Cell Interactions To Promote Cell-Cell HIV Spread

Paul Lopez,[a] Wan Hon Koh,[a] Ryan Hnatiuk,[a] Thomas T. Murooka[a,b]

[a]Department of Immunology, University of Manitoba, Winnipeg, Manitoba, Canada
[b]Department of Medical Microbiology and Infectious Disease, University of Manitoba, Winnipeg, Manitoba, Canada

ABSTRACT Macrophages are susceptible to HIV infection and play an important role in viral dissemination through cell-cell contacts with T cells. However, our current understanding of macrophage-to-T cell HIV transmission is derived from studies that do not consider the robust migration and cell-cell interaction dynamics between these cells. Here, we performed live-cell imaging studies in 3-dimensional (3D) collagen that allowed $CD4^+$ T cells to migrate and to locate and engage HIV-infected macrophages, modeling the dynamic aspects of the *in situ* environment in which these contacts frequently occur. We show that HIV^+ macrophages form stable contacts with $CD4^+$ T cells that are facilitated by both gp120-CD4 and LFA-1–ICAM-1 interactions and that prolonged contacts are a prerequisite for efficient viral spread. LFA-1–ICAM-1 adhesive contacts function to restrain highly motile T cells, since their blockade substantially destabilized macrophage-T cell contacts, resulting in abnormal tethering events that reduced cell-cell viral spread. HIV-infected macrophages displayed strikingly elongated podosomal extensions that were dependent on Nef expression but were dispensable for stable cell-cell contact formation. Finally, we observed persistent T cell infection in dynamic monocyte-derived macrophage (MDM)-T cell cocultures in the presence of single high antiretroviral drug concentrations but achieved complete inhibition with combination therapy. Together, our data implicate macrophages as drivers of T cell infection by altering physiological MDM-T cell contact dynamics to access and restrain large numbers of susceptible, motile T cells within lymphoid tissues.

IMPORTANCE Once HIV enters the lymphoid organs, exponential viral replication in T cells ensues. Given the densely packed nature of these tissues, where infected and uninfected cells are in nearly constant contact with one another, efficient HIV spread is thought to occur through cell-cell contacts *in vivo*. However, this has not been formally demonstrated. In this study, we performed live-cell imaging studies within a 3-dimensional space to recapitulate the dynamic aspects of the lymphoid microenvironment and asked whether HIV can alter the morphology, migration capacity, and cell-cell contact behaviors between macrophages and T cells. We show that HIV-infected macrophages can engage T cells in stable contacts through binding of virus- and host-derived adhesive molecules and that stable macrophage-T cell contacts were required for high viral spread. Thus, HIV alters physiological macrophage-T cell interactions in order to access and restrain large numbers of susceptible, motile T cells, thereby playing an important role in HIV progression.

KEYWORDS HIV, T cells, cell migration, cell-cell interactions, fluorescent reporters, live-cell imaging, macrophages

Secondary lymphoid organs (SLOs), such as the lymph nodes, orchestrate the adaptive immune response by coordinating the trafficking and intercellular communications between T cells and antigen-presenting cells (APCs) (1). The complex,

Citation Lopez P, Koh WH, Hnatiuk R, Murooka TT. 2019. HIV infection stabilizes macrophage-T cell interactions to promote cell-cell HIV spread. J Virol 93:e00805-19. https://doi.org/10.1128/JVI.00805-19.

Editor Frank Kirchhoff, Ulm University Medical Center

Address correspondence to Thomas T. Murooka, thomas.murooka@umanitoba.ca.

Received 14 May 2019
Accepted 25 June 2019
Accepted manuscript posted online 3 July 2019
Published 28 August 2019

3-dimensional (3D) meshwork of lymphoid stromal cells and reticular fibers within the T cell zone of the lymph node function to support T cell migration and facilitate interactions with APCs, which are also positioned on the same stromal networks (2, 3). This maximizes the frequency of APC-T cell contacts, which, in the absence of antigen recognition, remain short-lived and nonproductive. When T cells encounter cells presenting their cognate antigen in the context of the major histocompatibility complex (MHC), formation of a stable immunological synapse (IS) ensues. The IS activates a series of signaling cascades, which shape the differentiation and effector functions of ensuing T cell responses (4, 5). Thus, the abilities of immune cells to migrate through peripheral tissues and to engage in cell-cell interactions within SLOs are critical features of an effective immune surveillance program against invading pathogens.

Along with $CD4^+$ T cells, macrophages and microglial cells are targets of HIV infection *in vivo* and are associated with neurocognitive disorders and tissue pathology, especially during the late stages of AIDS, when T cells are depleted (6–11). Several distinct features of HIV replication in macrophages underscore their key role as potential viral reservoirs (12, 13), including (i) relative resistance to the cytopathic effects of HIV compared to T cells (14); (ii) harboring replication-competent virus for up to several weeks (15); (iii) residing within lymphoid tissues, where antiretroviral drug (ARV) penetration is reduced (16–18); and (iv) viral accumulation within surface-connected compartments (19–21) that are inaccessible to neutralizing antibodies (6). More recent studies using myeloid-only humanized mice (MoM) have demonstrated that myeloid cells can sustain high HIV production independently of T cells *in vivo* (22). Macrophage infection can persist during antiretroviral therapy (ART) and contribute to viral rebound after therapy interruption in a subset of MoM, implying an *in vivo* role of macrophages as important viral reservoirs (23). Furthermore, several studies have demonstrated that infected macrophages can transmit virus to T cells through direct cell-to-cell contact, leading to a substantially higher rate of T cell infection than cell-free virus alone (24–27). Cell-to-cell contacts facilitate simultaneous transfer of many viral particles, which reduces the blocking ability of certain classes of anti-Env neutralizing antibodies (28) and antiretroviral drugs (29), further contributing to the intense HIV replication observed in lymphoid tissues. Thus, while macrophages are less permissive to HIV-1 infection than activated $CD4^+$ T cells due to high SAMHD1 expression (30, 31), their localization and function as APCs may drive persistent T cell infection within SLOs through continuous cell-cell interactions.

One of the difficulties in evaluating previous studies that focus on the molecular aspects of cell-cell HIV transfer is the use of cell culture systems that do not consider the migratory behaviors and cell-cell interaction dynamics among leukocytes that normally occur within tissues. Whether HIV-associated adhesive molecular interactions are strong enough to cause T cell arrest and establish durable cell-cell interactions in a dynamic 3D environment remains an unanswered question. To address this, we performed live-cell microscopy within 3D collagen matrices (32–34) to visually characterize how HIV infection impacted dynamic macrophage-T cell interactions. We show that HIV infection of macrophages substantially enhances the frequency and duration of prolonged contacts with susceptible T cells and that both gp120-CD4 and LFA-1–ICAM-1 interactions are critical adhesive contacts that stabilize macrophage-T cell conjugates. Stable macrophage-T cell contacts were a prerequisite for efficient cell-cell viral transmission, which supported low levels of T cell infection even in the presence of single antiretroviral drugs at high concentrations. However, a combination of tenofovir (TDF), emtricitabine (FTC), and raltegravir (Ral) achieved complete viral replication inhibition, indicating that the drug regimen was sufficient to overcome the high multiplicity of cell-cell infection in our 3D model. Thus, our work better defines the dynamic interplay between cellular migration, cell morphology, and cell-cell interactions that collectively regulate cell-cell HIV spread and modulate antiretroviral drug efficacy.

RESULTS

Nef induces sustained morphological changes in HIV-infected macrophages. HIV-infected macrophages have increased numbers of cellular protrusions, or podosomes, that can degrade the extracellular matrix and enhance mesenchymal migration into various tissues (35). To further address whether these morphological changes can also impact HIV spread to T cells, we first performed live-cell imaging studies of monocyte-derived macrophages (MDMs) infected with either the wild type, HIV-GFP Δ*nef*, or HIV-GFP Δ*env* in collagen matrices. Macrophages infected with the wild type and HIV-GFP Δ*env*, but not HIV-GFP Δ*nef*, downregulated cell surface MHC-I expression, as expected (36) (Fig. 1B). To generate a relevant control population for all imaging studies, MDMs were transduced with a green fluorescent protein (GFP)-encoding lentivirus in parallel, yielding MDMs that expressed GFP at high levels comparable to those of their infected counterparts but lacking all viral protein expression (Fig. 1A). In a confined 3D environment, we observed that the control MDMs had a circular shape with short pseudopodial extensions that actively probed their surrounding space. In contrast, HIV infection drastically altered their morphology by promoting irregular cell shapes and cell protrusions that were sustained throughout the imaging period. These extended podosomes continued to actively probe their immediate environment, which significantly increased their total cell perimeters compared to uninfected macrophages. We confirmed that these morphological changes were the result of Nef expression, as macrophages infected with HIV-GFP Δ*nef* were phenotypically similar to uninfected cells, whereas infection with Env-deficient HIV also induced irregular cellular morphologies (Fig. 1C to E; see Video S1 in the supplemental material). The morphological changes were remarkably sustained over the course of the imaging studies, suggesting that Nef was continuously modulating actin polymerization to induce permanent phenotypic changes. Indeed, pretreatment with an inhibitor of Nef-mediated Src family kinase Hck activation completely reversed the formation of extended podosomes (Fig. 1F and G), confirming the results of a previous study (35). Similarly, HIV-infected "myeloid-like" cells were sessile and exhibited irregular morphologies and dynamic podosomal extensions in lymph nodes *in vivo* that were similar to those in collagen matrices (Fig. 1H and I; see Video S2 in the supplemental material). Together, the imaging studies confirmed that HIV infection induced drastic phenotypic changes in monocyte-derived macrophages that were entirely dependent on Nef expression. Notably, infected and uninfected macrophages were indistinguishable when plated onto two-dimensional (2D) tissue culture surfaces (data not shown), underscoring the emerging notion that *in vivo* cellular behaviors and functions are better recapitulated in confined 3D culture systems (37).

HIV-induced podosomes are not the result of syncytia or macrophage polarization. We postulated that macrophages with elongated podosomes could represent a subset of infected cells that had undergone cell-cell fusion or of syncytia (38, 39). To test this, we visualized the nuclei of infected macrophages using the HIV-nGFP reporter, where the nuclear localization signal was placed upstream of the GFP locus (nGFP), as described previously (40, 41). Live-cell imaging studies in collagen revealed that the vast majority (94.6%; $n = 41$) of infected macrophages had one discernible nucleus, indicating that syncytia, or multinuclear giant cells (MGCs), were not frequent at day 2 postinfection (Fig. 2A). When macrophage syncytia were observed, they had morphological features similar to those of mononucleated infected macrophages. Next, we addressed whether the observed morphological changes were influenced by macrophage polarization. After infecting unpolarized MDMs, the cells were cultured with either gamma interferon (IFN-γ) or interleukin 4 (IL-4) to polarize macrophages toward an M1 or M2a phenotype, respectively. The polarizing cytokines had an impact on subsequent HIV infection, consistent with previous studies (42), but not on cell circularity measurements (Fig. 2C and D). We observed a slight decrease in cell perimeter measurements in M2a macrophages, but elongated phenotypes remained prominent in this population, arguing that skewed polarization or cell-cell fusion does not explain the observed HIV-mediated morphological changes.

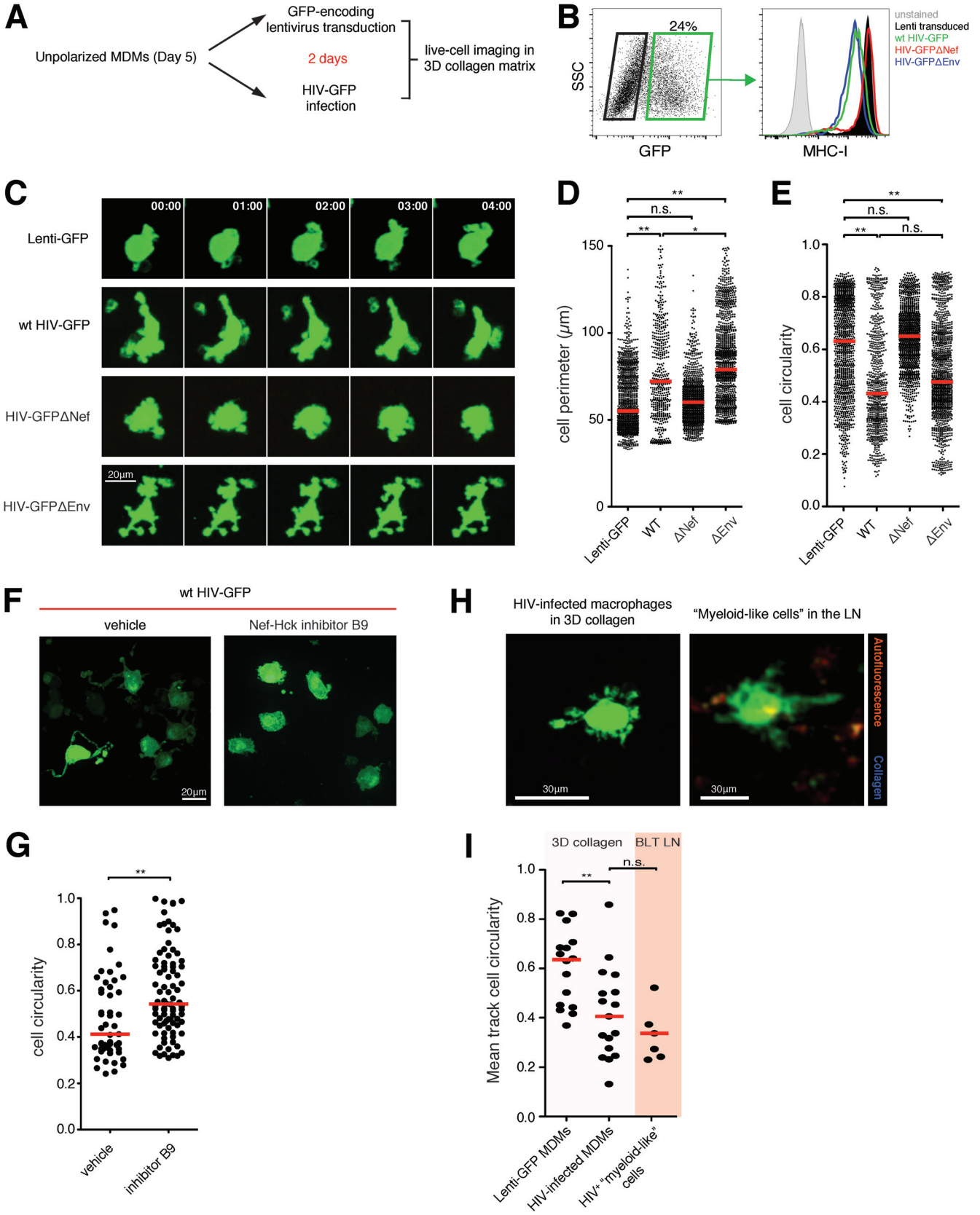

FIG 1 Nef induces sustained morphological changes in HIV-infected macrophages. (A) Experiment flow chart. (B) MDMs were infected either with the indicated HIV strains or with GFP-expressing lentivirus for 2 days and analyzed for GFP expression. Cell surface MHC-I expression in infected cells (green box) was compared to that in uninfected cells (black box). wt, wild type. (C) Time series micrograph of either uninfected or HIV-infected MDMs in 3D collagen matrices.

(Continued on next page)

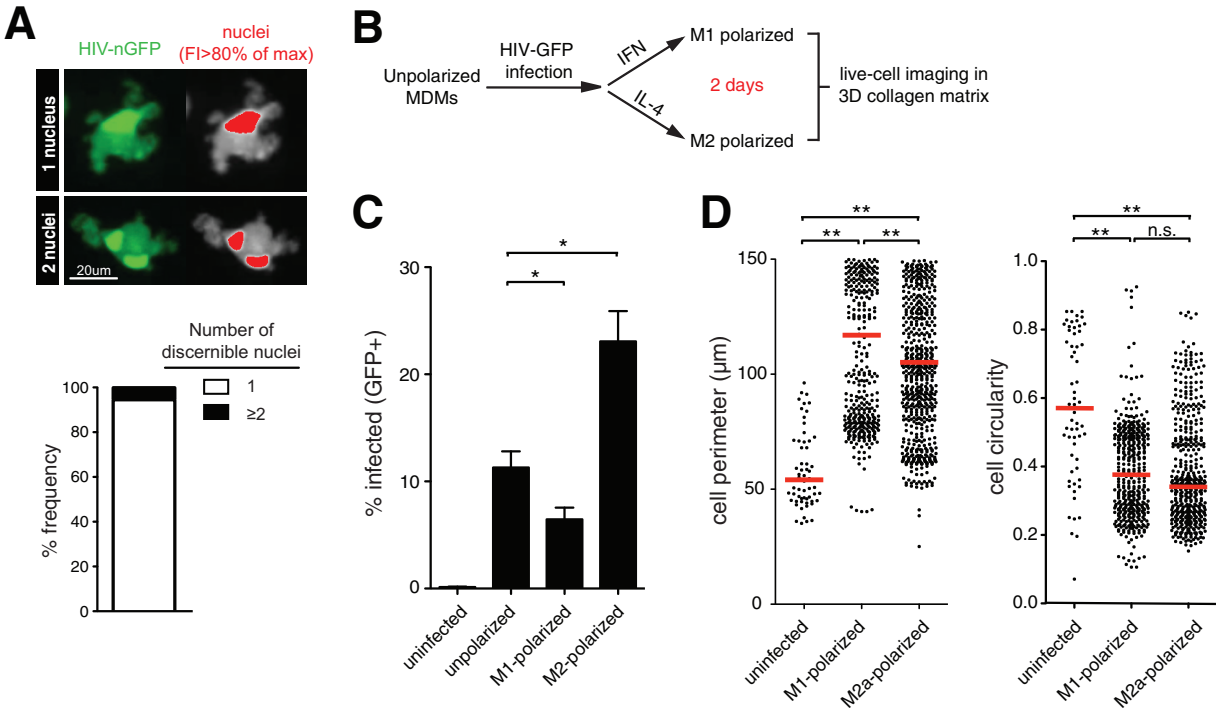

FIG 2 HIV-induced podosomes are not the result of syncytia or different macrophage polarization states. (A) (Left) Live-cell imaging micrograph of MDMs infected with HIV-nGFP for 2 days. (Right) Nuclei are indicated in red, based on an 80% maximum fluorescence intensity (FI) threshold. The frequency (percent) of infected MDMs ($n = 41$ cells) with one or more discernible nuclei is shown. (B) Experiment flow chart. (C) Percent GFP$^+$ MDMs at 2 days postinfection. Means and standard errors of the mean (SEM) are shown ($n = 3$). Statistical analysis was performed using a Mann-Whitney U test. *, $P < 0.01$. (D) Cell perimeter and circularity measurements. The red lines indicate median values. Statistical analysis was performed using a Mann-Whitney U test. **, $P < 0.001$; n.s., not significant.

Dynamic visualization of macrophage-T cell interactions in 3D collagen. HIV can be transmitted between cells at the site of adhesive contact, termed the virological synapse (VS). Cell-cell contacts between HIV-infected macrophages and susceptible T cells have been described (25, 26, 28) and can greatly enhance viral spread within cultures. Given that HIV infection of macrophages leads to modification of podosomes and a larger surface area, we hypothesized that these morphological changes can increase the frequency of T cell contacts and enhance viral transmission. To address this, we utilized a live-cell imaging approach by coembedding macrophages with autologous, *in vitro*-expanded CD4$^+$ T cells into a 3D collagen matrix (Fig. 3A). The T cells were highly motile in collagen, with migration speeds and behaviors comparable to those adoptively transferred into the lymph nodes of humanized mice (Fig. 3B and C). At steady state, contact between GFP-lentivirus (Lenti-GFP)-transduced control macrophages and T cells was transient (6 $\pm$ 3.8 min), whereas the addition of the superantigen staphylococcus enterotoxin B (SEB) significantly increased contact duration, as expected (Fig. 3D; see Video S3 in the supplemental material). Next, MDMs were infected with either HIV-GFP, HIV-GFP Δ*nef*, or HIV-GFP Δ*env* for 2 days before being coembedded with autologous CD4$^+$ T cells in collagen. Macrophages infected with wild-type HIV engaged in significantly prolonged contacts with T cells (15.50 $\pm$ 10 min),

FIG 1 Legend (Continued)
MDMs with HIV-induced podosomal extensions were observed. The time stamps are in minutes. (D and E) Cell perimeter (D) and cell circularity (E) measurements of infected MDMs. The red lines indicate median values. Statistical analysis was performed using a Mann-Whitney U test. *, $P < 0.05$; **, $P < 0.001$; n.s., not significant. (F) HIV-infected MDMs were treated either with vehicle alone or with 20 μM Nef-Hck activation inhibitor (B9) for 1 h prior to live-cell imaging studies in 3D collagen. Representative micrographs are shown. (G) Cell circularity measurements for both populations. The red bars indicate median values. **, $P < 0.01$. (H) Representative micrograph of HIV-infected macrophages (green) in collagen matrix or infected "myeloid-like" cells in the popliteal lymph node of a BLT mouse at day 6 postinfection. (I) Mean track cell circularity measurements of all infected cells in the different compartments. The red bars indicate median values. LN, lymph node; **, $P < 0.01$; n.s., not significant.

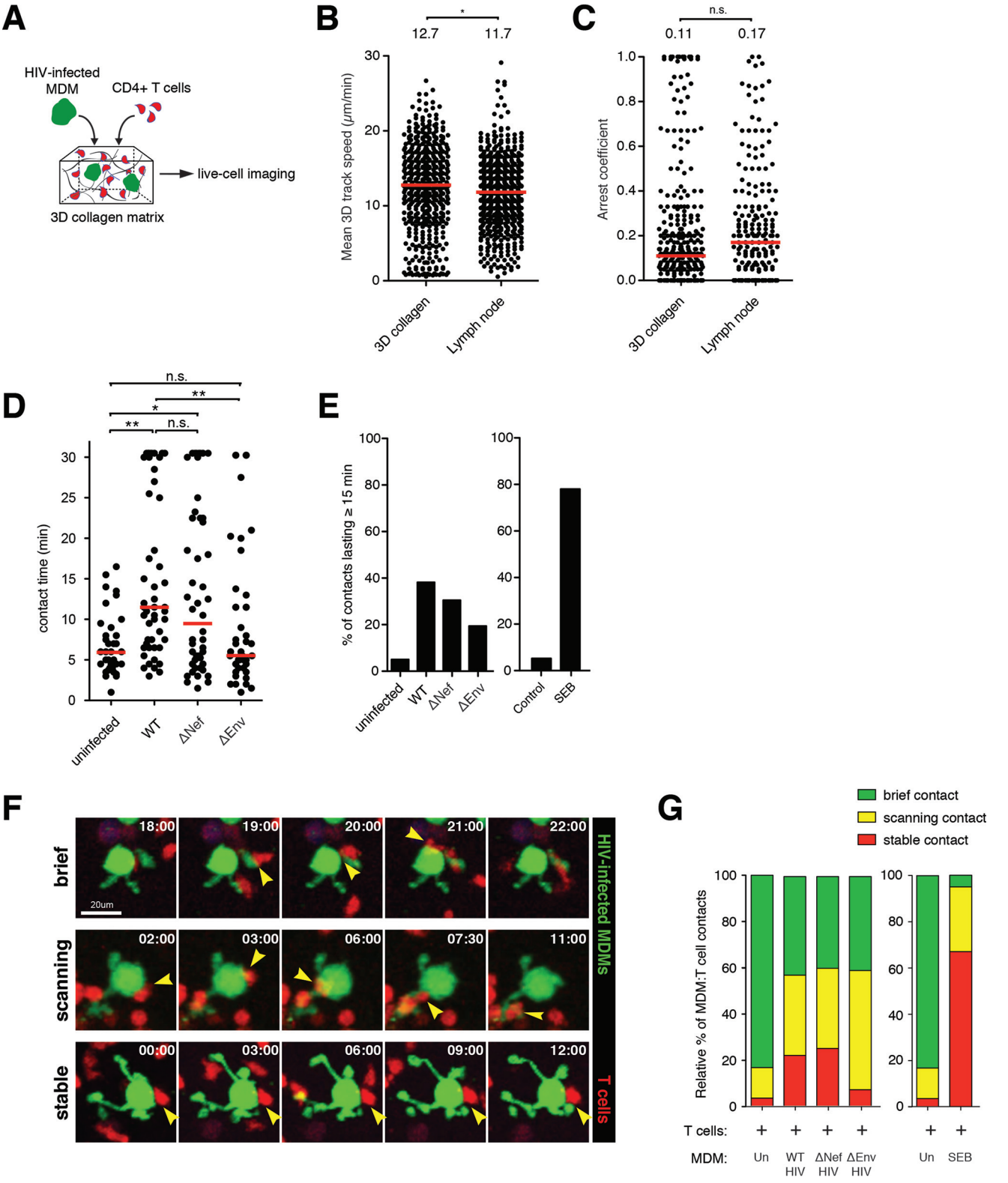

FIG 3 Dynamic visualization of macrophage-T cell interactions in 3D collagen. (A) Schematic of the experimental setup. HIV-GFP-infected MDMs (2 days) and CellTracker Orange CMTMR-labeled CD4$^+$ T cells were embedded into a collagen matrix and prepared for live-cell imaging studies. (B and C) Mean 3D track speed (B) and arrest coefficient values (C) for T cells migrating in two different media. The red bars indicate median values. Statistical analysis was performed using a Mann-Whitney U test. *, $P < 0.05$; n.s., not significant. (D) Durations of MDM-T cell contacts. The red lines indicate median values. Statistical analysis was performed using a Mann-Whitney U test. *, $P < 0.05$; **, $P < 0.01$; n.s., not significant. (E) Percent MDM-T cell contacts lasting more than 15 min. (F) Time series micrograph showing MDM-T cell contacts defined as stable, scanning, or brief. The arrowheads indicate the sites of cell-cell contact. The time stamps are in minutes. (G) Relative proportions of MDM-T cell contacts characterized as stable, scanning, and brief. Un, uninfected.

with ~40% of all macrophage-T cell contacts lasting more than 15 min. In contrast, less than 5% of control macrophages contacted T cells for greater than 15 min, whereas SEB induced stable interactions in the majority (~80%) of contacts. Surprisingly, the lack of Nef expression had no impact on average T cell contact times. This suggests that Nef-induced podosomal extensions were not involved in facilitating cell-cell interactions. Since macrophage-T cell interactions were highly dynamic, we further characterized these contacts into three distinct categories: brief contacts, with T cells migrating over 5 μm/min; scanning contacts, with T cells migrating between 2 and 5 μm/min; and stable contacts, with T cells migrating less than 2 μm/min (Fig. 3F; see Video S4 in the supplemental material). We show that a substantial proportion of T cells displayed either stable or scanning behavior while engaging infected MDMs compared to uninfected controls (Fig. 3G). Similar ratios were observed when macrophages were infected with HIV with *nef* deleted, confirming that Nef-induced podosomes had little impact on MDM-T cell contact dynamics. Collectively, our dynamic-imaging studies within a 3D matrix showed that HIV infection of macrophages promotes T cell arresting/scanning behaviors in over half of all macrophage-T cell encounters.

Role of Env in the formation of MDM-T cell conjugates. Env and CD4 molecules are enriched at the VS (28, 43, 44), but whether these interactions are solely responsible for facilitating stable macrophage-T cell contacts in a dynamic setting is not known. When MDMs were infected with HIV-GFP Δ*env* and coembedded with $CD4^+$ T cells in collagen, we observed an overall reduction in MDM-T cell contact duration (Fig. 3F and G) and a substantial skewing of stable T cell behavior to scanning T cell behavior, suggestive of destabilized macrophage-T cell conjugates (Fig. 3G). These data suggest that Env-CD4 interactions are important adhesive contacts for T cells as they migrate along the surfaces of macrophages, and they function to retain motile T cells. However, a significant proportion of T cells continued to display scanning behaviors even in the complete absence of Env expression, suggesting that other adhesive molecules may act in concert to facilitate prolonged macrophage-T cell conjugate formation.

Role of LFA-1–ICAM-1 interactions in stable MDM-T cell conjugate formation. The binding of LFA-1 and ICAM-1 has a well-characterized role in forming the IS and has also been described in VS formation (44–47). To determine whether LFA-1–ICAM-1 interactions are involved in stabilizing MDM-T cell contacts in a dynamic experimental setting, cells were pretreated with either isotype or neutralizing antibodies prior to coculture and imaging in collagen matrices (Fig. 4B). MDMs expressed high levels of ICAM-1 that were not altered by HIV infection, while activated $CD4^+$ T cells expressed LFA-1 (Fig. 4A). When both LFA-1 (on T cells) and ICAM-1 (on MDMs) were blocked with antibodies (blockade of >90%) (data not shown), we observed a reduced frequency of stable MDM-T cell contacts and a corresponding expansion of scanning behaviors compared to isotype antibody-treated cells (Fig. 4C). When the gp120-binding site of CD4 was blocked on T cells (blockade of >95%), a similar reduction in stable MDM-T cell conjugate frequencies was observed, consistent with earlier studies with the HIV-GFP Δ*env* mutant. Finally, when both Env-CD4 and LFA-1–ICAM-1 interactions were disrupted by integrin blockade, together with HIV-GFP Δ*env* infection, T cell contacts with macrophages were mostly brief, similar to uninfected controls. These data argue that both Env-CD4 and LFA-1–ICAM-1 adhesive contacts are mostly responsible for facilitating stable contacts between infected MDMs and T cells. Interestingly, disrupting LFA-1–ICAM-1 binding resulted in a marked increase in visible T cell-tethering events compared to isotype controls, where the uropodia of a migrating T cell remained physically attached to a macrophage by a membranous extension upon contact disengagement (Fig. 4D; see Video S5 in the supplemental material). When we defined a T cell-tethering event as one extending beyond 15 μm in length, we found that some MDM-T cell tethers reached over 40 μm. Tethering events were not observed between macrophages and T cells in the absence of HIV infection or when infected macrophages lacked Env expression (Fig. 4E and F). We also observed a large decrease in tethering events when both Env-CD4 and LFA-1–ICAM-1 interactions were absent, further implicating Env in tether formation. These data suggest that LFA-1–ICAM-1 interactions

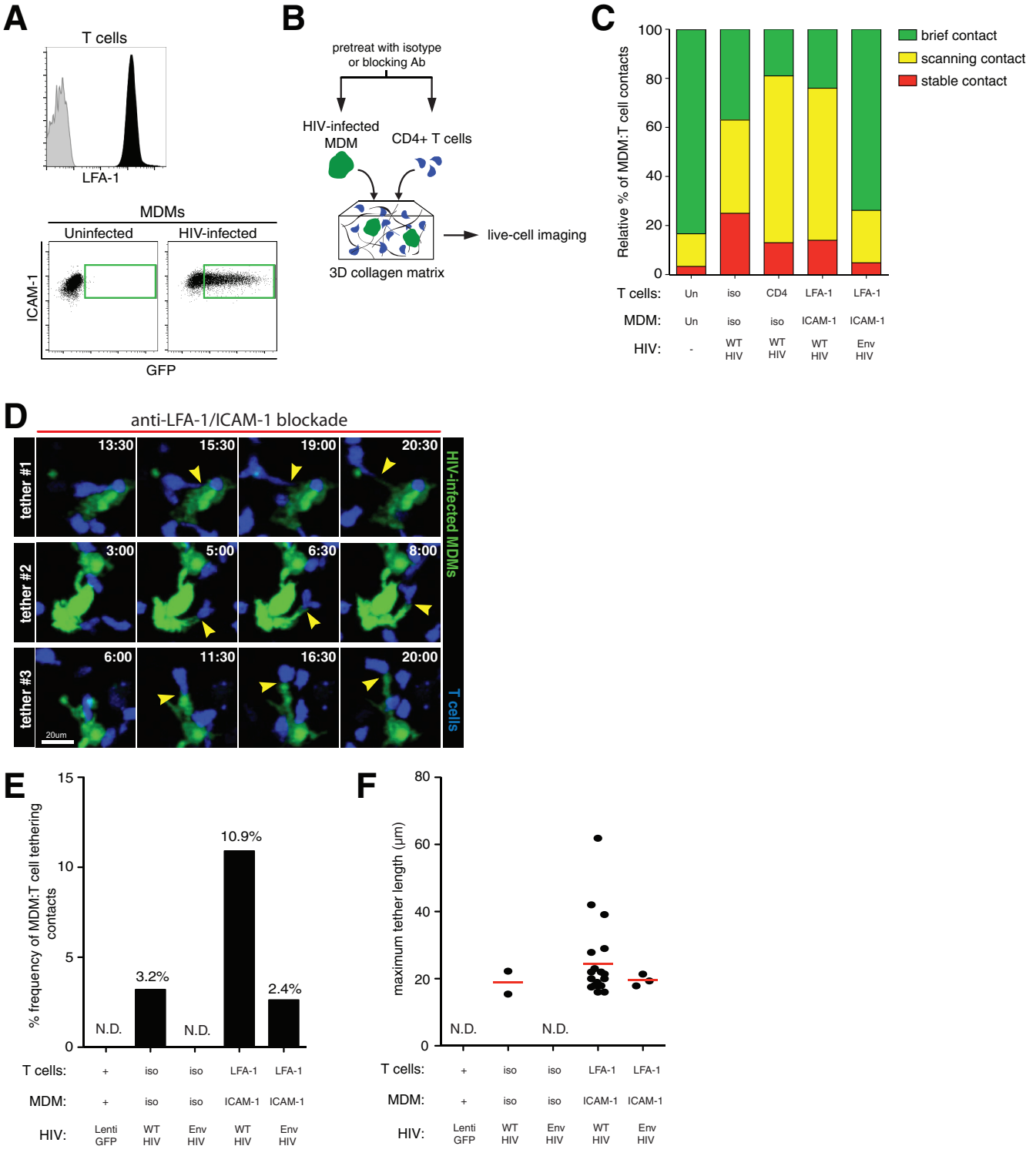

FIG 4 Role of adhesive molecular interactions in stabilizing MDM-T cell contacts during HIV infection. (A) Cell surface LFA-1 expression on T cells (black) and isotype control staining (gray). ICAM expression on MDMs after infection with HIV-GFP for 2 days is boxed in green. (B) Schematic of the experimental setup. HIV-GFP-infected MDMs and CMTMR-labeled CD4$^+$ T cells (blue) were pretreated with either isotype or the indicated blocking antibodies and embedded into a collagen matrix for live-cell imaging studies. (C) Relative proportions of MDM-T cell contacts characterized as stable, scanning, and brief. Blocking antibody conditions are indicated on the bottom axis. iso, isotype antibody. (D) Time series micrographs depicting three MDM-T cell-tethering events after LFA-1–ICAM-1 dual-antibody blockade. The arrowheads indicate the points of contact and the membranous tethers. The time stamps are in minutes. (E) Percent frequency of MDM-T cell-tethering events after specific antibody or isotype control blockade. Tethers were defined as membranous extensions between MDMs and T cells that were over 15 μm long. Frequency values (percent) are indicated above the bars. (F) Maximum tether lengths of MDM-T cell contacts. N.D., not detected.

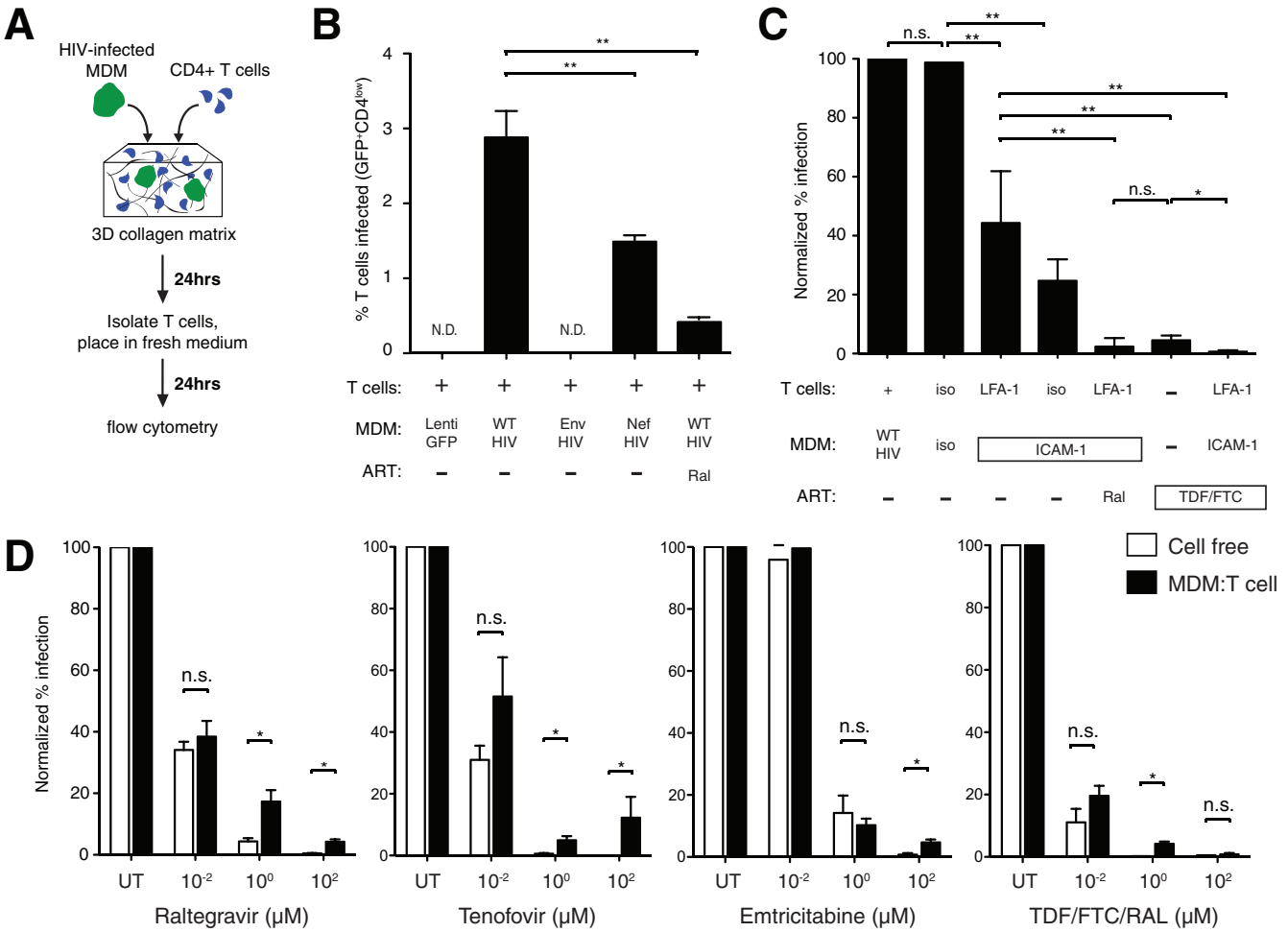

FIG 5 HIV dissemination through dynamic MDM-T cell interactions in collagen. (A) Schematic of the experimental setup. HIV-GFP-infected MDMs and CMAC-labeled CD4$^+$ T cells were coembedded into a collagen matrix for 24 h. The T cells were isolated and placed in fresh medium for an additional 24 h before analysis by flow cytometry. (B) Percentages of productively infected T cells, defined as GFP^{hi} CD4^{low}, after coculture in collagen under the specified conditions. Representative data from five donors are shown. Statistical analysis was performed using a Mann-Whitney U test. **, $P < 0.01$; N.D., not detected. (C) T cell infection after antibody blockade. Infection rates normalized to HIV$^+$ MDM-T cell cocultures are shown. iso, isotype control; Ral, 10 μM raltegravir; TDF-FTC, 10 μM each of tenofovir and emtricitabine. Representative data from four donors are shown. Statistical analysis was performed using a paired Student *t* test. *, $P < 0.05$; **, $P < 0.01$; n.s., not significant. (D) T cell infection after antiretroviral drug treatment under MDM-T cell or cell-free conditions in collagen. Infection rates normalized to untreated HIV$^+$ MDM-T cell cocultures are shown. TDF-FTC-Ral indicates combination therapy at the specified doses of each ARV. Statistical analysis was performed using a paired Student *t* test. *, $P < 0.05$; n.s., not significant.

helped stabilize macrophage-T cell contacts, which, if disrupted, failed to restrain T cells and resulted in abnormal tether formation.

Dynamic cell-cell HIV spread in 3D collagen. To examine how altered macrophage-T cell contact dynamics impact HIV dissemination, we developed a viral-spread assay where T cells were coembedded with HIV-GFP-infected MDMs in collagen for 24 h. T cells were isolated and incubated for a further 24-h period, where productively infected cells were defined as GFP$^+$ CD4^{low} cells that were also p24$^+$ by intracellular flow cytometry (Fig. 5A and data not shown). Of note, GFP$^+$ CD4^{hi} T cells contained small GFP blebs that were not productive infection and were excluded from our analysis. Productive T cell infection was observed in cocultures with HIV-infected MDMs, but not with Lenti-GFP-transduced or HIV-GFP Δ*env*-infected MDMs (Fig. 5B). The lack of Nef expression in macrophages reduced T cell infection by ~50%, consistent with the reduced infectivity of HIV Δ*nef* (48). We next focused on the impact of LFA-1–ICAM-1 blockade, given its negative impact on cell-cell stability and abnormal tether formation. We hypothesized that reducing the capacity of macrophages to restrain T cells would reduce viral-spread kinetics. Indeed, we observed a dramatic reduction in T cell

infection after dual anti-LFA-1–anti-ICAM-1 antibody blockade. Anti-ICAM-1 blockade alone was sufficient to reduce T cell infection to similar levels, suggesting that LFA-1 interacted primarily with ICAM-1 to facilitate HIV transmission (Fig. 5C). While TDF-FTC combination therapy significantly reduced T cell infection in this setting, dual-integrin blockade led to complete inhibition of T cell infection.

Antiretroviral drug efficacy during dynamic MDM-T cell HIV transmission. We next addressed whether dynamic cell-cell infection in collagen matrices impacted antiretroviral drug efficacy at different concentrations. In parallel with MDM-T cell cocultures, we infected T cells in collagen with 1.5×10^5 to 2.5×10^5 blue-forming units (bfu) cell-free HIV-GFP, which represents over 10 times the amount of cell-free HIV released by infected macrophages (data not shown). We tested raltegravir (an integrase inhibitor) and tenofovir and emtricitabine (both nucleotide analog reverse transcriptase inhibitors), either as single therapy or in combination (TDF-FTC-Ral), at different concentrations to assess the efficacy of ARVs in cell-cell versus cell-free infections in collagen chambers (Fig. 5D). At concentrations where cell-free HIV infection was completely suppressed, residual T cell infection ranging from 5 to 10% was observed for all three ARVs when given individually, even at 100 μM concentrations. When TDF-FTC-Ral at 1 μM of each ARV were added to cells, 4.2% $\pm$ 0.7% of T cells remained productively infected after coculture with infected MDMs, whereas complete inhibition of T cell infection was achieved when the same combinatory ARVs were given at 100 μM concentrations, demonstrating strong additive effects of three ARVs from two different therapeutic classes.

VCCs in elongated macrophages. In productively infected macrophages, HIV assembly and budding occur predominantly within surface-connected virus-containing compartments (VCCs) (21), although cell surface budding does occur (26). Given that HIV infection induces the formation of extensive podosomes, we next asked whether VCCs were located on these membranous extensions. We found that the use of Gag-iGFP reporters (carrying a Gag-internal, interdomain insertion of GFP) was not ideal to localize VCCs, since full-length Gag expression was found throughout the cell (reference 49 and data not shown). We therefore used an approach in which infected MDMs were fixed *in situ* in collagen gels with warmed 4% paraformaldehyde (PFA) overnight (Fig. 6A). This preserved the morphology of delicate podosomal extensions while allowing us to immunostain for mature VCCs using an anti-p17Gag antibody that detects only cleaved matrix (MA) protein. We observed that most VCCs, defined by bright p17Gag$^+$ clusters, were found in the cytoplasm and near the cell surface but almost never on podosomal extensions (Fig. 6B and C). When infected macrophages were cocultured with T cells, there was a substantial shift of p17Gag$^+$ clusters from intracellular compartments to the plasma membrane, suggesting that repeated interactions with T cells promotes VCC redistribution toward the cell surface.

DISCUSSION

Most studies examining cell-cell HIV transmission events have been performed using cell culture systems that do not allow cellular migration. For example, infected macrophages are plated on glass or plastic culture surfaces and overlaid with CD4$^+$ T cells for a defined period to assess T cell infection. In some cases, viral spread is measured under gentle shaking conditions to differentiate cell-free from cell-cell transmission by disrupting prolonged cellular contacts (24, 50). However, macrophage-T cell interactions *in vivo* are a dynamic process that is regulated by the natural propensity of T cells to migrate, cognate antigen recognition, and molecules that support cell-cell adhesion. HIV infection can drastically alter the motility and morphology of T cells and macrophages (35, 40, 41, 51), but how these changes impact cell-cell interaction dynamics within a confined 3D environment has not been studied. Our live-cell imaging approach within a collagen matrix allows T cells to migrate and to locate and engage infected macrophages to better model the main aspects of macrophage-T cell interaction dynamics within lymphoid tissues, where these contacts frequently occur. We show that both gp120-CD4 and LFA-1–ICAM-1 adhesive contacts play crucial roles in

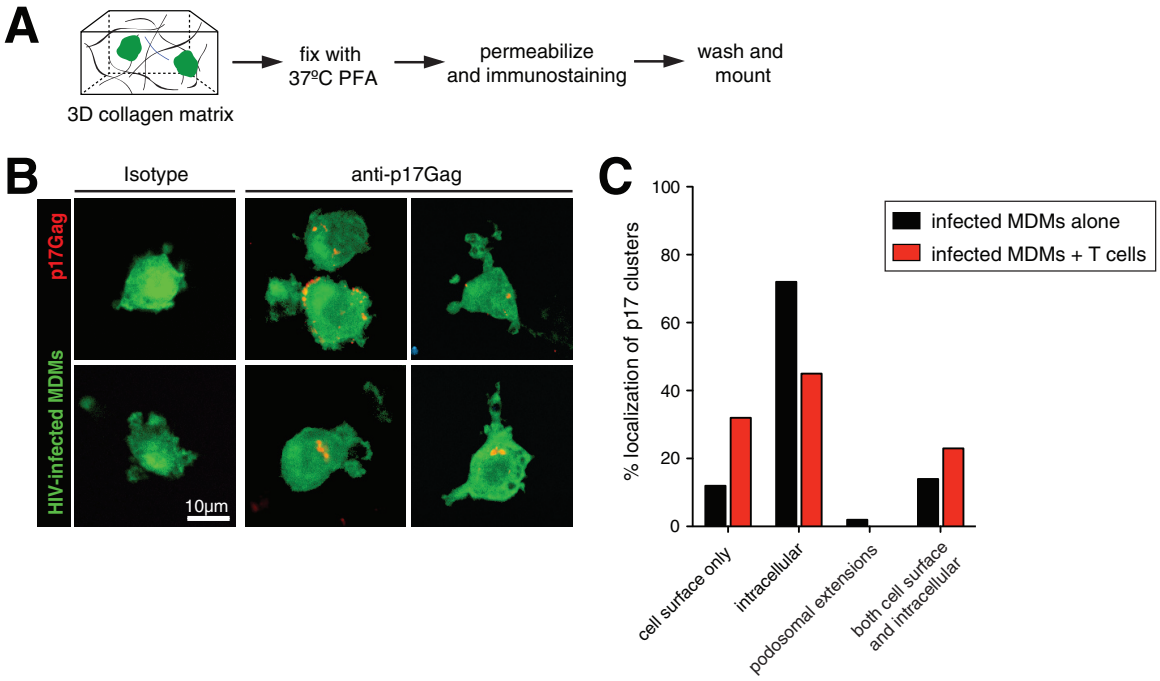

FIG 6 Localization of VCCs in HIV-infected macrophages. (A) Schematic of the experimental setup. HIV-GFP-infected MDMs (green) were incubated for 24 h in collagen and then fixed with paraformaldehyde. Gels were prepared for immunostaining with anti-p17Gag antibody. (B) Confocal micrographs of HIV-GFP-infected MDMs (green) stained with either isotype or anti-p17Gag antibody (red). Clusters of p17Gag staining represent VCCs. (C) Percent localization of p17Gag$^+$ VCCs in different regions of infected MDMs alone ($n = 43$) or after coculture with T cells ($n = 65$).

promoting T cell arrest and stabilizing macrophage-T cell contacts in this setting and that these stable interactions facilitate efficient viral spread. While residual T cell infection was observed in the presence of high single-ARV concentrations within MDM-T cell cocultures, combination therapy was able to achieve complete HIV suppression in this setting, highlighting the interplay between macrophage-to-T cell HIV spread dynamics and the ability of antiretrovirals to suppress this mode of viral spread.

We first assessed how HIV infection alters the morphology and behavior of monocyte-derived macrophages using our 3D collagen imaging approach. Consistent with previous studies (51), we observed highly dynamic podosomal extensions that continuously probed their immediate environment. Similar myeloid-like cells with active dendritic extensions were observed in the lymph nodes of humanized mice, although we were not able to definitively show that they were HIV-infected macrophages. These podosomes were largely dependent on Nef expression, which dramatically increased the cell perimeter and overall surface area of infected macrophages. Verollet and colleagues reported that HIV-induced modification of podosomes enhanced mesenchymal migration into various tissues by proteolytic degradation of the extracellular matrix as one possible mechanism of viral dissemination (35, 52). This involved activation of the Nef-Hck signaling axis and the downstream WASP pathway (53). We further extended these findings by addressing whether podosome modifications were enhanced by cell-cell fusions or syncytia (also referred to as MGCs) (38, 39). MGCs of myeloid origin have been reported in the lymphoid tissues, colons, and brains of AIDS patients (54, 55) and associated with HIV-induced encephalopathy (56–58). We also observed large myeloid-like MGCs in the lymph nodes of BLT humanized mice (59, 60). However, we observed only a small proportion of infected macrophages that had more than one discernible nucleus after infection with HIV-nGFP. While our assessment of fusion events was limited to 2 days postinfection, it is clear that macrophage syncytia can occur at later time points (38). We also ruled out the skewing of macrophage polarization as a possible explanation. Collectively, these data argue that the observed

Nef-induced morphological changes were a general phenomenon of macrophages and not explained by cell-cell fusion or altered polarization states.

We reasoned that Nef-induced podosome formation could increase viral spread in at least two ways: (i) enhanced capacity to migrate into and within tissues can deliver HIV to susceptible cells, such as those in the intestinal mucosa (35), and (ii) active probing of podosomes can restrain and transmit HIV to more T cells. We took advantage of the fact that Nef was exclusively responsible for podosome formation and addressed their role in cell-cell viral transmission. Unexpectedly, the lack of Nef expression had little impact on T cell contact duration but did reduce productive T cell infection, likely due to the ability of Nef to enhance viral infectivity and replication without altering MDM-T cell contact dynamics (48). Additionally, VCCs containing mature virus were almost never found on podosomes, unlike HIV particles, which were present on the tips of viral filopodial extensions of infected dendritic cells (DCs) (61). Thus, we propose that virus-induced podosomes in macrophages likely contribute to HIV pathogenesis by modulating migration or other cellular functions, such as phagocytosis or cytokine release (62–65).

Using our dynamic-imaging approach, we addressed how HIV infection impacted macrophage-T cell interactions and how these contacts translate to viral dissemination. It is well established that Env-CD4 interactions can drive the formation of the virological synapse (43, 44, 66), but whether these adhesive contacts are sufficiently strong to restrain motile T cells is not known. HIV gp120 engagement of the CD4 molecule could deliver a stop signal to arrest T cell motility and induce VS assembly on planar lipid bilayers, but these responses were dependent on gp120 density (46). Whether the cell surface expression/density of gp120 on infected macrophages is sufficient to cause T cell arrest has not been tested. The preferential assembly and budding of HIV within intracellular compartments could mean that less gp120 is available on the cell surface than on infected T cells (20, 21). Our imaging studies showed that HIV infection significantly enhanced T cell dwell times, where approximately 60% of T cells analyzed displayed either scanning or stopping behavior upon contact with an infected macrophage. When Env expression was abolished, a marked reduction in contact duration and frequency of arrested T cells was observed, suggestive of destabilized macrophage-T cell contacts. Pretreatment with anti-CD4 antibodies prior to coculture similarly led to contact destabilization, implying that sufficient cell surface gp120 was present to engage and restrain motile T cells. The ability of gp120 to induce T cell arrest is reminiscent of antigen-induced T cell arrest mediated by calcium signaling downstream of the T cell receptor (TCR). A clear difference is the duration of the resulting contacts; unlike cell-cell contacts after TCR engagement, which last for hours (4, 67), the HIV-induced contacts observed here were more transient. This is in line with the transient nature of MDM-T cell (25, 28) and T cell-T cell (68) VSs in cocultures and on lipid bilayers (46) but contrast with studies that show T cell-T cell VSs lasting for hours to days (49). Whether sustained cell-cell contacts would persist under conditions where cell motility is considered was not addressed in these studies. There are also conflicting data regarding the signals that cause T cell arrest: soluble gp120 could induce Ca^{2+} flux in a chemokine receptor-dependent manner (69), but not in another study using bound gp120, even though T cells were arrested (70). These data seem to indicate that calcium flux may be dependent on the nature of gp120-CD4 binding and that other signaling pathways regulate cell-cell interactions during infection. Cell surface molecules known to be enriched at the VS, including CD81 tetraspanin (26), GM1 ganglioside (71), and integrins (44, 47), can further regulate cell-cell interactions and fine-tune signals across the VS. Receptors involved in antigen recognition, such as MHC-II, CD80/CD86, and CD28, may facilitate both priming and infection of HIV-specific CD4 T cells through cell-cell contacts (72, 73). Finally, chemokine binding has been shown to disrupt gp120-CD4 interactions, indirectly modulating macrophage-T cell conjugate formation (46). Interestingly, a recent study demonstrated that motile kinapse formations, defined as mobile scanning contacts, were sufficient to prime human $CD4^+$ T cells *in vitro*, arguing that stable APC-T cell conjugates are not an absolute requirement for antigenic

priming (74). It is plausible, then, that macrophage-T cell scanning behaviors are similar to motile kinapses and are facilitated by signals generated through gp120-CD4 interactions. Together, HIV takes advantage of physiological macrophage-T cell interactions to maximize access to a large number of susceptible T cells, mainly through expression of cell surface gp120.

The virological and immunological synapses are both stabilized by an LFA-1–ICAM-1 ring that surrounds the central TCR-MHC and gp120-CD4 clusters, respectively (45, 75, 76). While gp120-mediated T cell arrest facilitates the formation of stable macrophage-T cell conjugates, LFA-1 is also enriched at the VS (44, 47). Upon ligand binding, the cytoplasmic tail of the β2 subunit contributes to outside-in signaling to fully activate the high-affinity conformation of LFA-1 (77). Antibody blockade of the β2 subunit had no impact on 3D T cell migration (data not shown) but led to a reduction in the proportion of stable macrophage-T cell contacts, suggesting their partial role in stabilizing cell-cell contacts. Strikingly, we observed an increase in MDM-T cell-tethering events after LFA-1–ICAM-1 dual blockade, where a thin membranous extension from macrophages could be seen to remain attached to the uropodia of migrating T cells after contact disengagement, some reaching over 40 μm in length. Our imaging studies also clearly showed that tethers were not formed between stable MDM-T cell contacts, but rather, they became visible when T cells appeared to dissociate contact with infected macrophages. This resulted in motile T cells creating membranous tethers that became "stretched" between T cells and infected macrophages, followed by a sudden release of contact. We found that tether formation was dependent on Env expressed by infected macrophages. We also noted that the observed tethers were GFP positive, indicating that the membranous tethers were derived from infected, GFP-expressing macrophages. These data, together with the fact that both Env-CD4 and LFA-1–ICAM-1 interactions facilitate prolonged MDM-T cell contacts, suggest that tethering events are the result of macrophages being unable to "restrain" migratory T cells. Blockade of LFA-1–ICAM-1 contacts while leaving Env-CD4 contacts intact may reduce the ability of macrophages to restrain T cells, which in our 3D setting contributed to cell-cell tethers. This is also supported by the fact that LFA-1 blockade led to a significant reduction in T cell infection in MDM-T cell cocultures. LFA-1–ICAM-1 integrins (and ICAM-3) are enriched at the VS (44, 47), and disrupting their binding reduces VS assembly and cell-cell viral transmission (28, 47, 66). LFA-1 ligation promotes T cell polarization and microtubule-organizing center (MTOC) reorganization toward the cell-cell contact site (78), further supporting the idea that integrins function to regulate the nature of cell-cell interactions during VS formation. Macrophage-T cell tethers are reminiscent of previously described membrane nanotubes (79) and filopodial bridges (80) between infected and uninfected cells, which can facilitate the transfer of HIV particles. Similar tethers between macrophages and B cells have been described as a conduit for Nef exchange *in vivo* (81). However, the MDM-T cell tethers observed here are unlikely to facilitate viral transfer, since they were associated with reduced HIV spread. While the anti-ICAM-1 antibody has been shown to reduce infection by cell-free HIV that bears host-derived ICAM-1 on the cell surface (82), we rule out this possibility, since antibody access into VCCs is very limited, given the very low rate of diffusion through the narrow surface-connected conduits (19). It is important to also mention that some tethering events, albeit at very low frequencies, were observed in the absence of Env and integrin binding (Fig. 4E and F). It is possible that other adhesive contacts also play a role in MDM-T cell tethering or, alternatively, that binding of anti-LFA-1 (or ICAM-1) antibody may induce signaling through receptor cross-linking and directly modulating T cell behaviors. Future genetic approaches will be used to further refine the molecular aspects of MDM-T cell interaction dynamics.

The simultaneous transfer of virus at a high multiplicity of infection (MOI) at the site of cell contact is a central feature of cell-cell HIV transmission, lowering the efficacy of some classes of ARVs when given as monotherapies (29, 83–85). Reduced potency of nucleoside analog reverse transcriptase inhibitors (NRTIs) is also observed when T cells are infected with cell-free virus at a high MOI, which seems to suggest that the large

number of incoming viruses, rather than the physical requirements of cell-cell contacts, are the main determinant of NRTI monotherapy potency (83). However, cell-cell interactions can initiate specific signaling pathways that enhance VS formation, increase viral spread, and help establish latent T cell infection, even in the absence of cognate antigen recognition (86–88). These data argue that the molecular architecture of the viral synapse provides signals that impact the context in which target cells encounter transmitted virus and alter their susceptibility to infection. Our imaging studies highlight the importance of assessing ARV potency within a 3D setting, especially as combination therapy, where physiological on/off contact dynamics between infected macrophages and T cells may impact viral spread kinetics and ARV efficacy. We assessed whether combining the NRTIs tenofovir (TFV) and emtricitabine (ETC), which are less effective at blocking cell-cell HIV spread, with an integrase inhibitor, raltegravir, would enhance viral suppression in our 3D model. TFV, ETC, and raltegravir, given individually at concentrations that completely inhibited cell-free HIV infection, exhibited reduced potency in MDM-T cell cocultures, where T cell infection rates of 5 to 10% were detected at the highest doses tested, in line with a previous study (24). In contrast, complete suppression was achieved when MDM-T cell cocultures were treated with TDF-FTC-Ral, consistent with the notion that combination therapy significantly improves drug efficacy against efficient cell-cell transmission (83, 84). Combining nucleotide analogs has been shown to enhance their ability to terminate the growing DNA chain (89), while suppressive activity against cell-cell spread of HIV was further enhanced with an antiretroviral drug from another therapeutic class. Thus, our data show that the combination regimen tested was sufficient to overcome the high multiplicity of cell-cell infection observed in our 3D model. Additionally, blocking LFA-1–ICAM-1 interactions had an additive effect on TDF-FTC activity, albeit a modest one, indicating that, in principle, ARV efficacy can be further enhanced by disrupting prolonged contacts between infected and uninfected cells. This has implications for our understanding of cell-cell transmission events *in vivo*, where immune cells are in nearly constant contact with one another within lymphoid tissues, where lower drug penetration has been documented (16, 17).

In conclusion, our imaging studies presented here contrast with previous studies by taking into account the dynamic aspects of macrophage-T cell interactions during HIV infection within a confined 3D matrix environment. We show that infected macrophages promote both prolonged scanning and stable contacts with motile T cells that are stabilized by gp120-CD4 and LFA-1–ICAM-1 interactions and that such stable contacts are a prerequisite for efficient T cell infection. While Nef-induced morphological changes were not responsible for enhancing cell-cell interactions or viral spread, complete inhibition of macrophage-to-T cell viral spread was achieved with combinatory ARV regimens tested in our model. The fact that macrophages can be infected by engulfing infected T cells (90) or through transcytosis (91), in addition to their ability to capture virions from surrounding cells (92, 93), strongly argues that lymph node macrophages are important players in HIV dissemination through their propensity to contact numerous susceptible T cells *in vivo*.

MATERIALS AND METHODS

HIV and lentiviral plasmids. The lentiviral vector construct pHAGE-CMV-GFP (94) was packaged with standard helper and vesicular stomatitis virus G protein (VSVg)-encoding plasmids to obtain GFP-expressing lentiviral stocks. The construction of HIV-nGFP has been described previously (40). The SIV3+ plasmid was used to generate VLP-Vpx. The proviral plasmid pBR-NL43-IRES-EGFP-*nef*$^+$ (pleG-*nef*$^+$) was obtained from the NIH AIDS Research and Reference Reagent Program (catalog no. 11349). The V3 loop of *env* was modified to resemble that of HIV BaL and to confer R5 tropism and was designated HIV-GFP (40). To generate a strain with *nef* deleted, HIV-GFP was digested with MluI and XhoI and religated using T4 DNA polymerase and quick ligase (NEB; catalog no. E0542L) (designated HIV-GFP Δ*nef*). The HIV plasmid with *env* deleted was constructed by digesting the HIV-GFP plasmid with PsiI to generate a frameshift mutation, as described previously (40).

Preparation of HIV and lentiviral stocks. All HIV-1 stocks were produced by transient transfection of HEK 293T cells (ATCC; CRL-3216) using calcium phosphate. An expression plasmid encoding VSVg was used to produce VSVg-pseudotyped HIV. Viral supernatants were collected 48 h after transfection and centrifuged at 32,000 rpm for 1.5 h using an SW70Ti rotor (Beckman Coulter) over a 20% sucrose cushion.

Viral stocks were titrated using MAGI.CCR5 and expressed as bfu per milliliter. To produce ΔNef and ΔEnv HIV, their respective proviral plasmids were constructed and transfected into HEK 293T cells. To ensure one round of infection, the ΔEnv HIV strain was pseudotyped with VSVg.

Cell culture and HIV infection. Human CD14$^+$ monocytes and CD4$^+$ T cells (Stem Cell Technologies) were isolated from the peripheral blood mononuclear cell (PBMC) fraction of healthy donors (NetCAD; Canadian Blood Services). Cell purities for both populations were routinely >95%. Monocytes were differentiated into macrophages by seeding into tissue culture (Thermo Fisher; catalog no. 174951) with 50 ng/ml human recombinant macrophage colony-stimulating factor (hrM-CSF) (Biolegend; catalog no. 574808) in RPMI 1640 supplemented with 10% fetal bovine serum (FBS) (VWR Seradigm; catalog no. 1500-500), 2 mM GlutaMAX (Gibco; catalog no. 3050-061), 1 mM sodium pyruvate (Corning; catalog no. 25-000-CI), and 10 mM HEPES (Sigma-Aldrich; catalog no. H4034) for at least 5 days. In some cases, MDMs were detached using Accutase (Biolegend; catalog no. 423201) and further cultured in ultra-low-attachment culture flasks (Thermo Fisher; catalog no. 174951). Naïve CD4$^+$ T cells were activated by adding Dynabeads coated with anti-human CD3ε/CD28 antibody (1:1 bead/cell ratio; Life Technologies; catalog no. 11131D) in complete RPMI 1640. After 2 days, the beads were removed, and the cells were cultured for another 6 to 8 days in medium containing 50 IU/ml human recombinant IL-2 (rIL-2) (Peprotech; catalog no. 200-02), keeping cell density close to 2×10^5 cells/ml. The cells were used for all experiments between days 7 and 10. To infect MDMs, cells were first preincubated with VLP-Vpx for 3 h at 6×10^6 cells/ml in the presence of 8 μg/ml Polybrene, 100 ng/ml rhM-CSF and infected under the same conditions with HIV for an additional 2 to 3 h. The cells were kept in culture in the presence of 25 ng/ml rhM-CSF for the specified times. Infection was measured by GFP expression using flow cytometry. In some studies, an inhibitor of Nef-mediated Hck activation was used at 20 mM concentrations (Calbiochem; catalog no. 500653). All work with human blood was approved by the University of Manitoba Biomedical Research Ethics Board (BREB).

Flow cytometry. Phenotypic characterization of T cells and MDMs was performed on the LSRII (Becton, Dickinson) using FlowJo software (Tree Star) for analysis. T cells and MDMs were washed, counted, and stained with a panel of directly conjugated anti-human monoclonal antibodies (MAbs): MHCI-APC (allophycocyanin) (W6/32), CD4-APC (RPA-T4), and CD3-APC/Cy7 (HIT3a). Intracellular p24 staining (Beckman Coulter; KC57) was used to measure HIV infection within GFP-positive cells. HIV-infected cells were fixed with 2.5% PFA for 30 min before flow cytometry analysis.

Live-cell imaging in 3D collagen chambers. Collagen type I, which is a major constituent of most interstitial tissues, was used to recreate the 3D fibrillar networks in SLOs. Glass slide chambers were constructed as previously described (95). MDMs were either infected with HIV-GFP or transduced with GFP-expressing lentivirus before resuspension in a collagen-medium solution. Bovine collagen (PureCol; catalog no. 5005) was used to achieve a final concentration of 1.7 mg/ml in each chamber. In some experiments, T cells were labeled with Celltracker Blue (CMAC; 15 μM) prior to coculture with macrophages in collagen at an MDM/T cell ratio of 1:2. For blockade studies, cells were pretreated with 3 μg of either isotype or blocking antibodies per 10^6 cells prior to embedding into collagen gels. For blocking antibodies, anti-LFA-1 β-chain (BD Biosciences; L130), anti-CD4 (Biolegend; RPA-T4), and anti-ICAM-1 (BD Biosciences; LB-2) were used. To prevent FcR-mediated opsonization, MDMs were pretreated with FcR blocker (Biolegend; catalog no. 422302). The chambers were allowed to solidify for 45 min at 37°C-5% CO_2 and placed onto a custom-made heating platform attached to a temperature controller apparatus (Werner Instruments). A multiphoton microscope with two Ti-sapphire lasers (Coherent) was tuned to between 780 and 920 nm for optimized excitation of the fluorescent probes used. For four-dimensional recordings of cell migration, stacks of 12 optical sections (512 by 512 pixels) with 4-μm z-spacing were acquired every 15 (or 30) seconds to provide imaging volumes 44 μm in depth. Emitted light was detected through 460/50-nm, 525/70-nm, and 595/50-nm dichroic filters with nondescanned detectors. All images were acquired using a 20× 1.0-numerical-aperture (NA) Olympus objective lens (XLUMPLFLN; 2.0-mm working distance [WD]).

Image analysis. Data sets were transformed in Imaris 8.3 (Bitplane) to generate maximum-intensity projections (MIPs) for export as Quicktime movies. Automated 3D tracking of T cell centroids was performed for motility analyses. Further cell track parameters (arrest coefficient and mean displacement) were analyzed in Matlab (Mathworks). To measure the macrophage surface area and cell perimeters, image data sets were imported into ImageJ (NIH), and each cell was traced using the wand (tracing) tool after color thresholding. Circularity (on a scale between 0 and 1, where 0 is a straight line and 1 indicates a perfect circle) measurements were performed using ImageJ. Contact duration, cell migration speeds during contacts, and tethering lengths were all analyzed using ImageJ. Tether length was defined as the longest distance from which a visible membranous tether from the cell body of infected MDMs to a contacting T cell could be observed. ImageJ was used to categorize HIV clusters as near the cell surface (<2 μm from the cell surface), intracellular (>2 μm from the cell surface), or on podosomal extensions.

Cell-free and cell-associated HIV spread in 3D collagen matrix. One million HIV-infected MDMs and 2×10^6 T cells were embedded into 270 μl of collagen gel supplemented with rhIL-2 and rhM-CSF and placed into 48-well plates. After 4 to 5 h, 150 μl of complete RPMI 1640 medium supplemented with IL-2 and M-CSF was overlaid on the solidified gel and incubated for 24 h. The collagen gels were digested with collagenase D, and then the cells were washed and resuspended in medium with IL-2 in a 6-well plate. In order to remove MDMs, T cells in suspension were removed after 2 to 3 h and placed in a new 6-well plate, while the adherent MDMs remained on the plate (which removed >95% of the MDMs). The T cells were incubated for another 24 h before flow cytometric analysis for productive HIV infection. To assess infection by cell-free virus, 1.5×10^5 to 2.5×10^5 IU of HIV-GFP was incubated with T cells

immediately prior to collagen embedding. This represented an infecting virus dose of more than 10 times the viral titer produced by infected macrophages over 2 days in culture (data not shown). In some experiments, cells were pretreated with either isotype control or blocking antibodies prior to and during cocultures in collagen. When antiretroviral drugs were used, T cells were pretreated with the specified concentrations of Ral, TDF, and/or FTC for 30 min prior to and during coculture with MDMs in collagen.

Immunohistochemistry in 3D collagen gels. Collagen gels containing 1 million HIV-infected MDMs alone or cocultured with 4×10^6 CMAC-labeled T cells were embedded and solidified in a 24-well plate for 2 to 3 h in a 37°C incubator. The collagen block was fixed with prewarmed 4% PFA-5% sucrose in phosphate-buffered saline (PBS) solution overnight at 37°C. Excess PFA was quenched using 0.1 M glycine solution (Sigma) and then permeabilized using 0.5% Triton X-100 (Sigma) for 48 h. To prevent nonspecific binding, the collagen block was incubated with 1% bovine serum albumin (BSA) and Fc blocker overnight. A monoclonal antibody against HIV-1 p17 (ATCC; HB-8975) was added to the gels for 24 h, followed by an Alexa Fluor 568-labeled secondary antibody (Thermo Fisher; catalog no. 1793903). The labeled gel block was mounted onto a glass slide and imaged with a Zeiss spinning-disk confocal microscope using ZEN software.

Statistical analysis. The unpaired Student *t* test and Mann-Whitney U test were used for comparison of data sets with normal and nonnormal distributions, respectively, using Prism 6 (GraphPad). Medians and *P* values from statistical analyses are indicated in each graph. When *P* values were larger than 0.05, differences were considered not significant.

Ethics statement. Anonymized donor cells from healthy subjects were obtained through NetCAD (approval no. nc0005) and approved by the University of Manitoba BREB (no. B2015:030). Informed written consent was collected by NetCAD, and anonymized cells were used for this study.

SUPPLEMENTAL MATERIAL

Supplemental material for this article may be found at https://doi.org/10.1128/JVI.00805-19.

SUPPLEMENTAL FILE 1, MOV file, 11.3 MB.
SUPPLEMENTAL FILE 2, MOV file, 7.9 MB.
SUPPLEMENTAL FILE 3, MOV file, 11 MB.
SUPPLEMENTAL FILE 4, MOV file, 3 MB.
SUPPLEMENTAL FILE 5, MOV file, 17.9 MB.
SUPPLEMENTAL FILE 6, PDF file, 0.1 MB.

ACKNOWLEDGMENTS

We thank Eric Cohen and Mariana Bego (Univérsite de Montréal) for generously providing us with anti-p17 antibody and Thorsten Mempel (Massachusetts General Hospital) for providing us with reagents and imaging data from BLT mice. Cells, drugs, and viruses were received from the National Institute of Health AIDS Reagent Program.

This work was supported in part by a Canadian Institute for Health Research (CIHR) project grant, CIHR-funded Canadian HIV Cure Enterprise (CanCURE) Team Grant HB2-164064 (T.T.M.), and Research Manitoba (T.T.M.). W.H.K. holds a postdoctoral fellow award from Research Manitoba.

P.L., W.H.K., and T.T.M. conceived and designed the experiments; P.L., W.H.K., and R.H. performed the experiments; P.L., W.H.K., and T.T.M. analyzed the data; P.L. and T.T.M. wrote the manuscript.

We declare no competing financial interests.

REFERENCES

1. Mempel TR, Junt T, von Andrian UH. 2006. Rulers over randomness: stroma cells guide lymphocyte migration in lymph nodes. Immunity 25:867–869. https://doi.org/10.1016/j.immuni.2006.11.002.
2. Bajenoff M, Egen JG, Koo LY, Laugier JP, Brau F, Glaichenhaus N, Germain RN. 2006. Stromal cell networks regulate lymphocyte entry, migration, and territoriality in lymph nodes. Immunity 25:989–1001. https://doi.org/10.1016/j.immuni.2006.10.011.
3. Bajenoff M, Granjeaud S, Guerder S. 2003. The strategy of T cell antigen-presenting cell encounter in antigen-draining lymph nodes revealed by imaging of initial T cell activation. J Exp Med 198:715–724. https://doi.org/10.1084/jem.20030167.
4. Mempel TR, Henrickson SE, von Andrian UH. 2004. T-cell priming by dendritic cells in lymph nodes occurs in three distinct phases. Nature 427:154–159. https://doi.org/10.1038/nature02238.
5. Henrickson SE, Mempel TR, Mazo IB, Liu B, Artyomov MN, Zheng H, Peixoto A, Flynn MP, Senman B, Junt T, Wong HC, Chakraborty AK, von Andrian UH. 2008. T cell sensing of antigen dose governs interactive behavior with dendritic cells and sets a threshold for T cell activation. Nat Immunol 9:282–291. https://doi.org/10.1038/ni1559.
6. Koppensteiner H, Banning C, Schneider C, Hohenberg H, Schindler M. 2012. Macrophage internal HIV-1 is protected from neutralizing antibodies. J Virol 86:2826–2836. https://doi.org/10.1128/JVI.05915-11.
7. Gendelman HE, Orenstein JM, Martin MA, Ferrua C, Mitra R, Phipps T, Wahl LA, Lane HC, Fauci AS, Burke DS. 1988. Efficient isolation and propagation of human immunodeficiency virus on recombinant colony-stimulating factor 1-treated monocytes. J Exp Med 167:1428–1441. https://doi.org/10.1084/jem.167.4.1428.
8. Orenstein JM. 2001. The macrophage in HIV infection. Immunobiology 204:598–602. https://doi.org/10.1078/0171-2985-00098.
9. Lewin-Smith M, Wahl SM, Orenstein JM. 1999. Human immunodeficiency

virus-rich multinucleated giant cells in the colon: a case report with transmission electron microscopy, immunohistochemistry, and in situ hybridization. Mod Pathol 12:75–81.
10. Churchill MJ, Deeks SG, Margolis DM, Siliciano RF, Swanstrom R. 2016. HIV reservoirs: what, where and how to target them. Nat Rev Microbiol 14:55–60. https://doi.org/10.1038/nrmicro.2015.5.
11. Gray LR, On H, Roberts E, Lu HK, Moso MA, Raison JA, Papaioannou C, Cheng WJ, Ellett AM, Jacobson JC, Purcell DF, Wesselingh SL, Gorry PR, Lewin SR, Churchill MJ. 2016. Toxicity and in vitro activity of HIV-1 latency-reversing agents in primary CNS cells. J Neurovirol 22:455–463. https://doi.org/10.1007/s13365-015-0413-4.
12. Brown A, Zhang H, Lopez P, Pardo CA, Gartner S. 2006. In vitro modeling of the HIV-macrophage reservoir. J Leukoc Biol 80:1127–1135. https://doi.org/10.1189/jlb.0206126.
13. Le Douce V, Herbein G, Rohr O, Schwartz C. 2010. Molecular mechanisms of HIV-1 persistence in the monocyte-macrophage lineage. Retrovirology 7:32. https://doi.org/10.1186/1742-4690-7-32.
14. Swingler S, Mann AM, Zhou J, Swingler C, Stevenson M. 2007. Apoptotic killing of HIV-1-infected macrophages is subverted by the viral envelope glycoprotein. PLoS Pathog 3:1281–1290. https://doi.org/10.1371/journal.ppat.0030134.
15. Sharova N, Swingler C, Sharkey M, Stevenson M. 2005. Macrophages archive HIV-1 virions for dissemination in trans. EMBO J 24:2481–2489. https://doi.org/10.1038/sj.emboj.7600707.
16. Fletcher CV, Staskus K, Wietgrefe SW, Rothenberger M, Reilly C, Chipman JG, Beilman GJ, Khoruts A, Thorkelson A, Schmidt TE, Anderson J, Perkey K, Stevenson M, Perelson AS, Douek DC, Haase AT, Schacker TW. 2014. Persistent HIV-1 replication is associated with lower antiretroviral drug concentrations in lymphatic tissues. Proc Natl Acad Sci U S A 111:2307–2312. https://doi.org/10.1073/pnas.1318249111.
17. Martinez-Picado J, Deeks SG. 2016. Persistent HIV-1 replication during antiretroviral therapy. Curr Opin HIV AIDS 11:417–423. https://doi.org/10.1097/COH.0000000000000287.
18. Sigal A, Baltimore D. 2012. As good as it gets? The problem of HIV persistence despite antiretroviral drugs. Cell Host Microbe 12:132–138. https://doi.org/10.1016/j.chom.2012.07.005.
19. Welsch S, Keppler OT, Habermann A, Allespach I, Krijnse-Locker J, Kräusslich H-G. 2007. HIV-1 buds predominantly at the plasma membrane of primary human macrophages. PLoS Pathog 3:e36. https://doi.org/10.1371/journal.ppat.0030036.
20. Deneka M, Pelchen-Matthews A, Byland R, Ruiz-Mateos E, Marsh M. 2007. In macrophages, HIV-1 assembles into an intracellular plasma membrane domain containing the tetraspanins CD81, CD9, and CD53. J Cell Biol 177:329–341. https://doi.org/10.1083/jcb.200609050.
21. Nkwe DO, Pelchen-Matthews A, Burden JJ, Collinson LM, Marsh M. 2016. The intracellular plasma membrane-connected compartment in the assembly of HIV-1 in human macrophages. BMC Biol 14:50. https://doi.org/10.1186/s12915-016-0272-3.
22. Honeycutt JB, Wahl A, Baker C, Spagnuolo RA, Foster J, Zakharova O, Wietgrefe S, Caro-Vegas C, Madden V, Sharpe G, Haase AT, Eron JJ, Garcia JV. 2016. Macrophages sustain HIV replication in vivo independently of T cells. J Clin Invest 126:1353–1366. https://doi.org/10.1172/JCI84456.
23. Honeycutt JB, Thayer WO, Baker CE, Ribeiro RM, Lada SM, Cao Y, Cleary RA, Hudgens MG, Richman DD, Garcia JV. 2017. HIV persistence in tissue macrophages of humanized myeloid-only mice during antiretroviral therapy. Nat Med 23:638–643. https://doi.org/10.1038/nm.4319.
24. Duncan CJ, Russell RA, Sattentau QJ. 2013. High multiplicity HIV-1 cell-to-cell transmission from macrophages to CD4+ T cells limits antiretroviral efficacy. AIDS 27:2201–2206. https://doi.org/10.1097/QAD.0b013e3283632ec4.
25. Groot F, Welsch S, Sattentau QJ. 2008. Efficient HIV-1 transmission from macrophages to T cells across transient virological synapses. Blood 111:4660–4663. https://doi.org/10.1182/blood-2007-12-130070.
26. Gousset K, Ablan SD, Coren LV, Ono A, Soheilian F, Nagashima K, Ott DE, Freed EO. 2008. Real-time visualization of HIV-1 GAG trafficking in infected macrophages. PLoS Pathog 4:e1000015. https://doi.org/10.1371/journal.ppat.1000015.
27. Carr JM, Hocking H, Li P, Burrell CJ. 1999. Rapid and efficient cell-to-cell transmission of human immunodeficiency virus infection from monocyte-derived macrophages to peripheral blood lymphocytes. Virology 265:319–329. https://doi.org/10.1006/viro.1999.0047.
28. Duncan CJ, Williams JP, Schiffner T, Gartner K, Ochsenbauer C, Kappes J, Russell RA, Frater J, Sattentau QJ. 2014. High-multiplicity HIV-1 infection and neutralizing antibody evasion mediated by the macrophage-T cell virological synapse. J Virol 88:2025–2034. https://doi.org/10.1128/JVI.03245-13.
29. Sigal A, Kim JT, Balazs AB, Dekel E, Mayo A, Milo R, Baltimore D. 2011. Cell-to-cell spread of HIV permits ongoing replication despite antiretroviral therapy. Nature 477:95–98. https://doi.org/10.1038/nature10347.
30. Laguette N, Sobhian B, Casartelli N, Ringeard M, Chable-Bessia C, Segeral E, Yatim A, Emiliani S, Schwartz O, Benkirane M. 2011. SAMHD1 is the dendritic- and myeloid-cell-specific HIV-1 restriction factor counteracted by Vpx. Nature 474:654–657. https://doi.org/10.1038/nature10117.
31. Hrecka K, Hao C, Gierszewska M, Swanson SK, Kesik-Brodacka M, Srivastava S, Florens L, Washburn MP, Skowronski J. 2011. Vpx relieves inhibition of HIV-1 infection of macrophages mediated by the SAMHD1 protein. Nature 474:658–661. https://doi.org/10.1038/nature10195.
32. Friedl P, Noble PB, Zanker KS. 1995. T lymphocyte locomotion in a three-dimensional collagen matrix. J Immunol 154:4973–4985.
33. Gunzer M, Schafer A, Borgmann S, Grabbe S, Zanker KS, Brocker EB, Kampgen E, Friedl P. 2000. Antigen presentation in extracellular matrix: interactions of T cells with dendritic cells are dynamic, short lived, and sequential. Immunity 13:323–332. https://doi.org/10.1016/S1074-7613(00)00032-7.
34. Wolf K, Muller R, Borgmann S, Brocker EB, Friedl P. 2003. Amoeboid shape change and contact guidance: T-lymphocyte crawling through fibrillar collagen is independent of matrix remodeling by MMPs and other proteases. Blood 102:3262–3269. https://doi.org/10.1182/blood-2002-12-3791.
35. Verollet C, Souriant S, Bonnaud E, Jolicoeur P, Raynaud-Messina B, Kinnaer C, Fourquaux I, Imle A, Benichou S, Fackler OT, Poincloux R, Maridonneau-Parini I. 2015. HIV-1 reprograms the migration of macrophages. Blood 125:1611–1622. https://doi.org/10.1182/blood-2014-08-596775.
36. Piguet V, Schwartz O, Le Gall S, Trono D. 1999. The downregulation of CD4 and MHC-I by primate lentiviruses: a paradigm for the modulation of cell surface receptors. Immunol Rev 168:51–63. https://doi.org/10.1111/j.1600-065X.1999.tb01282.x.
37. Lämmermann T, Bader BL, Monkley SJ, Worbs T, Wedlich-Söldner R, Hirsch K, Keller M, Förster R, Critchley DR, Fässler R, Sixt M. 2008. Rapid leukocyte migration by integrin-independent flowing and squeezing. Nature 453:51–55. https://doi.org/10.1038/nature06887.
38. Verollet C, Zhang YM, Le Cabec V, Mazzolini J, Charriere G, Labrousse A, Bouchet J, Medina I, Biessen E, Niedergang F, Benichou S, Maridonneau-Parini I. 2010. HIV-1 Nef triggers macrophage fusion in a p61Hck- and protease-dependent manner. J Immunol 184:7030–7039. https://doi.org/10.4049/jimmunol.0903345.
39. Bracq L, Xie M, Lambele M, Vu LT, Matz J, Schmitt A, Delon J, Zhou P, Randriamampita C, Bouchet J, Benichou S. 2017. T cell-macrophage fusion triggers multinucleated giant cell formation for HIV-1 spreading. J Virol. https://doi.org/10.1128/JVI.01237-17.
40. Murooka TT, Deruaz M, Marangoni F, Vrbanac VD, Seung E, von Andrian UH, Tager AM, Luster AD, Mempel TR. 2012. HIV-infected T cells are migratory vehicles for viral dissemination. Nature 490:283–287. https://doi.org/10.1038/nature11398.
41. Symeonides M, Murooka TT, Bellfy LN, Roy NH, Mempel TR, Thali M. 2015. HIV-1-induced small T cell syncytia can transfer virus particles to target cells through transient contacts. Viruses 7:6590–6603. https://doi.org/10.3390/v7122959.
42. Cassol E, Cassetta L, Rizzi C, Alfano M, Poli G. 2009. M1 and M2a polarization of human monocyte-derived macrophages inhibits HIV-1 replication by distinct mechanisms. J Immunol 182:6237–6246. https://doi.org/10.4049/jimmunol.0803447.
43. Chen P, Hubner W, Spinelli MA, Chen BK. 2007. Predominant mode of human immunodeficiency virus transfer between T cells is mediated by sustained Env-dependent neutralization-resistant virological synapses. J Virol 81:12582–12595. https://doi.org/10.1128/JVI.00381-07.
44. Jolly C, Kashefi K, Hollinshead M, Sattentau QJ. 2004. HIV-1 cell to cell transfer across an Env-induced, actin-dependent synapse. J Exp Med 199:283–293. https://doi.org/10.1084/jem.20030648.
45. Vasiliver-Shamis G, Dustin ML, Hioe CE. 2010. HIV-1 virological synapse is not simply a copycat of the immunological synapse. Viruses 2:1239–1260. https://doi.org/10.3390/v2051239.
46. Vasiliver-Shamis G, Tuen M, Wu TW, Starr T, Cameron TO, Thomson R, Kaur G, Liu J, Visciano ML, Li H, Kumar R, Ansari R, Han DP, Cho MW, Dustin ML, Hioe CE. 2008. Human immunodeficiency virus type 1 envelope gp120 induces a stop signal and virological synapse formation in

noninfected CD4+ T cells. J Virol 82:9445–9457. https://doi.org/10.1128/JVI.00835-08.
47. Jolly C, Mitar I, Sattentau QJ. 2007. Adhesion molecule interactions facilitate human immunodeficiency virus type 1-induced virological synapse formation between T cells. J Virol 81:13916–13921. https://doi.org/10.1128/JVI.01585-07.
48. Munch J, Rajan D, Schindler M, Specht A, Rucker E, Novembre FJ, Nerrienet E, Muller-Trutwin MC, Peeters M, Hahn BH, Kirchhoff F. 2007. Nef-mediated enhancement of virion infectivity and stimulation of viral replication are fundamental properties of primate lentiviruses. J Virol 81:13852–13864. https://doi.org/10.1128/JVI.00904-07.
49. Hubner W, McNerney GP, Chen P, Dale BM, Gordon RE, Chuang FY, Li XD, Asmuth DM, Huser T, Chen BK. 2009. Quantitative 3D video microscopy of HIV transfer across T cell virological synapses. Science 323:1743–1747. https://doi.org/10.1126/science.1167525.
50. Sourisseau M, Sol-Foulon N, Porrot F, Blanchet F, Schwartz O. 2007. Inefficient human immunodeficiency virus replication in mobile lymphocytes. J Virol 81:1000–1012. https://doi.org/10.1128/JVI.01629-06.
51. Verollet C, Le Cabec V, Maridonneau-Parini I. 2015. HIV-1 infection of T lymphocytes and macrophages affects their migration via Nef. Front Immunol 6:514. https://doi.org/10.3389/fimmu.2015.00514.
52. Wiesner C, Le-Cabec V, El Azzouzi K, Maridonneau-Parini I, Linder S. 2014. Podosomes in space: macrophage migration and matrix degradation in 2D and 3D settings. Cell Adh Migr 8:179–191. https://doi.org/10.4161/cam.28116.
53. Cougoule C, Le Cabec V, Poincloux R, Al Saati T, Mege JL, Tabouret G, Lowell CA, Laviolette-Malirat N, Maridonneau-Parini I. 2010. Three-dimensional migration of macrophages requires Hck for podosome organization and extracellular matrix proteolysis. Blood 115:1444–1452. https://doi.org/10.1182/blood-2009-04-218735.
54. Frankel SS, Wenig BM, Burke AP, Mannan P, Thompson LD, Abbondanzo SL, Nelson AM, Pope M, Steinman RM. 1996. Replication of HIV-1 in dendritic cell-derived syncytia at the mucosal surface of the adenoid. Science 272:115–117. https://doi.org/10.1126/science.272.5258.115.
55. Dargent JL, Lespagnard L, Kornreich A, Hermans P, Clumeck N, Verhest A. 2000. HIV-associated multinucleated giant cells in lymphoid tissue of the Waldeyer's ring: a detailed study. Mod Pathol 13:1293–1299. https://doi.org/10.1038/modpathol.3880237.
56. Sharer LR, Cho ES, Epstein LG. 1985. Multinucleated giant cells and HTLV-III in AIDS encephalopathy. Hum Pathol 16:760. https://doi.org/10.1016/S0046-8177(85)80245-8.
57. Sharer LR, Epstein LG, Cho ES, Joshi VV, Meyenhofer MF, Rankin LF, Petito CK. 1986. Pathologic features of AIDS encephalopathy in children: evidence for LAV/HTLV-III infection of brain. Hum Pathol 17:271–284. https://doi.org/10.1016/S0046-8177(83)80220-2.
58. Kato T, Hirano A, Llena JF, Dembitzer HM. 1987. Neuropathology of acquired immune deficiency syndrome (AIDS) in 53 autopsy cases with particular emphasis on microglial nodules and multinucleated giant cells. Acta Neuropathol 73:287–294. https://doi.org/10.1007/BF00686624.
59. Murooka TT, Sharaf RR, Mempel TR. 2015. Large syncytia in lymph nodes induced by CCR5-tropic HIV-1. AIDS Res Hum Retroviruses 31:471–472. https://doi.org/10.1089/aid.2014.0378.
60. Compton AA, Schwartz O. 2017. They might be giants: does syncytium formation sink or spread HIV infection?. PLoS Pathog 13:e1006099. https://doi.org/10.1371/journal.ppat.1006099.
61. Aggarwal A, Iemma TL, Shih I, Newsome TP, McAllery S, Cunningham AL, Turville SG. 2012. Mobilization of HIV spread by diaphanous 2 dependent filopodia in infected dendritic cells. PLoS Pathog 8:e1002762. https://doi.org/10.1371/journal.ppat.1002762.
62. Kumar A, Herbein G. 2014. The macrophage: a therapeutic target in HIV-1 infection. Mol Cell Ther 2:10. https://doi.org/10.1186/2052-8426-2-10.
63. Mazzolini J, Herit F, Bouchet J, Benmerah A, Benichou S, Niedergang F. 2010. Inhibition of phagocytosis in HIV-1-infected macrophages relies on Nef-dependent alteration of focal delivery of recycling compartments. Blood 115:4226–4236. https://doi.org/10.1182/blood-2009-12-259473.
64. Le-Bury G, Niedergang F. 2018. Defective phagocytic properties of HIV-infected macrophages: how might they be implicated in the development of invasive Salmonella Typhimurium? Front Immunol 9:531. https://doi.org/10.3389/fimmu.2018.00531.
65. Herbein G, Mahlknecht U, Batliwalla F, Gregersen P, Pappas T, Butler J, O'Brien WA, Verdin E. 1998. Apoptosis of CD8+ T cells is mediated by macrophages through interaction of HIV gp120 with chemokine receptor CXCR4. Nature 395:189–194. https://doi.org/10.1038/26026.
66. Rudnicka D, Feldmann J, Porrot F, Wietgrefe S, Guadagnini S, Prevost MC, Estaquier J, Haase AT, Sol-Foulon N, Schwartz O. 2009. Simultaneous cell-to-cell transmission of human immunodeficiency virus to multiple targets through polysynapses. J Virol 83:6234–6246. https://doi.org/10.1128/JVI.00282-09.
67. Miller MJ, Wei SH, Cahalan MD, Parker I. 2003. Autonomous T cell trafficking examined in vivo with intravital two-photon microscopy. Proc Natl Acad Sci U S A 100:2604–2609. https://doi.org/10.1073/pnas.2628040100.
68. Groppelli E, Starling S, Jolly C. 2015. Contact-induced mitochondrial polarization supports HIV-1 virological synapse formation. J Virol 89:14–24. https://doi.org/10.1128/JVI.02425-14.
69. Melar M, Ott DE, Hope TJ. 2007. Physiological levels of virion-associated human immunodeficiency virus type 1 envelope induce coreceptor-dependent calcium flux. J Virol 81:1773–1785. https://doi.org/10.1128/JVI.01316-06.
70. Vasiliver-Shamis G, Cho MW, Hioe CE, Dustin ML. 2009. Human immunodeficiency virus type 1 envelope gp120-induced partial T-cell receptor signaling creates an F-actin-depleted zone in the virological synapse. J Virol 83:11341–11355. https://doi.org/10.1128/JVI.01440-09.
71. Jolly C, Sattentau QJ. 2005. Human immunodeficiency virus type 1 virological synapse formation in T cells requires lipid raft integrity. J Virol 79:12088–12094. https://doi.org/10.1128/JVI.79.18.12088-12094.2005.
72. Douek DC, Brenchley JM, Betts MR, Ambrozak DR, Hill BJ, Okamoto Y, Casazza JP, Kuruppu J, Kunstman K, Wolinsky S, Grossman Z, Dybul M, Oxenius A, Price DA, Connors M, Koup RA. 2002. HIV preferentially infects HIV-specific CD4+ T cells. Nature 417:95–98. https://doi.org/10.1038/417095a.
73. Lore K, Smed-Sorensen A, Vasudevan J, Mascola JR, Koup RA. 2005. Myeloid and plasmacytoid dendritic cells transfer HIV-1 preferentially to antigen-specific CD4+ T cells. J Exp Med 201:2023–2033. https://doi.org/10.1084/jem.20042413.
74. Mayya V, Judokusumo E, Abu Shah E, Peel CG, Neiswanger W, Depoil D, Blair DA, Wiggins CH, Kam LC, Dustin ML. 2018. Durable interactions of T cells with T cell receptor stimuli in the absence of a stable immunological synapse. Cell. Rep 22:340–349. https://doi.org/10.1016/j.celrep.2017.12.052.
75. Bromley SK, Burack WR, Johnson KG, Somersalo K, Sims TN, Sumen C, Davis MM, Shaw AS, Allen PM, Dustin ML. 2001. The immunological synapse. Annu Rev Immunol 19:375–396. https://doi.org/10.1146/annurev.immunol.19.1.375.
76. Jolly C, Sattentau QJ. 2004. Retroviral spread by induction of virological synapses. Traffic 5:643–650. https://doi.org/10.1111/j.1600-0854.2004.00209.x.
77. Hogg N, Patzak I, Willenbrock F. 2011. The insider's guide to leukocyte integrin signalling and function. Nat Rev Immunol 11:416–426. https://doi.org/10.1038/nri2986.
78. Starling S, Jolly C. 2016. LFA-1 engagement triggers T cell polarization at the HIV-1 virological synapse. J Virol 90:9841–9854. https://doi.org/10.1128/JVI.01152-16.
79. Sowinski S, Jolly C, Berninghausen O, Purbhoo MA, Chauveau A, Kohler K, Oddos S, Eissmann P, Brodsky FM, Hopkins C, Onfelt B, Sattentau Q, Davis DM. 2008. Membrane nanotubes physically connect T cells over long distances presenting a novel route for HIV-1 transmission. Nat Cell Biol 10:211–219. https://doi.org/10.1038/ncb1682.
80. Sherer NM, Lehmann MJ, Jimenez-Soto LF, Horensavitz C, Pypaert M, Mothes W. 2007. Retroviruses can establish filopodial bridges for efficient cell-to-cell transmission. Nat Cell Biol 9:310–315. https://doi.org/10.1038/ncb1544.
81. Qiao X, He B, Chiu A, Knowles DM, Chadburn A, Cerutti A. 2006. Human immunodeficiency virus 1 Nef suppresses CD40-dependent immunoglobulin class switching in bystander B cells. Nat Immunol 7:302–310. https://doi.org/10.1038/ni1302.
82. Fortin JF, Cantin R, Lamontagne G, Tremblay M. 1997. Host-derived ICAM-1 glycoproteins incorporated on human immunodeficiency virus type 1 are biologically active and enhance viral infectivity. J Virol 71:3588–3596.
83. Agosto LM, Zhong P, Munro J, Mothes W. 2014. Highly active antiretroviral therapies are effective against HIV-1 cell-to-cell transmission. PLoS Pathog 10:e1003982. https://doi.org/10.1371/journal.ppat.1003982.
84. Titanji BK, Pillay D, Jolly C. 2017. Combination antiretroviral therapy and cell-cell spread of wild-type and drug-resistant human immunodeficiency virus-1. J Gen Virol 98:821–834. https://doi.org/10.1099/jgv.0.000728.

85. Titanji BK, Aasa-Chapman M, Pillay D, Jolly C. 2013. Protease inhibitors effectively block cell-to-cell spread of HIV-1 between T cells. Retrovirology 10:161. https://doi.org/10.1186/1742-4690-10-161.
86. Len ACL, Starling S, Shivkumar M, Jolly C. 2017. HIV-1 activates T cell signaling independently of antigen to drive viral spread. Cell Rep 18:1062–1074. https://doi.org/10.1016/j.celrep.2016.12.057.
87. Kumar NA, van der Sluis RM, Mota T, Pascoe R, Evans VA, Lewin SR, Cameron PU. 2018. Myeloid dendritic cells induce HIV latency in proliferating CD4(+) T cells. J Immunol 201:1468–1477. https://doi.org/10.4049/jimmunol.1701233.
88. Evans VA, Kumar N, Filali A, Procopio FA, Yegorov O, Goulet JP, Saleh S, Haddad EK, da Fonseca Pereira C, Ellenberg PC, Sekaly RP, Cameron PU, Lewin SR. 2013. Myeloid dendritic cells induce HIV-1 latency in non-proliferating CD4+ T cells. PLoS Pathog 9:e1003799. https://doi.org/10.1371/journal.ppat.1003799.
89. Feng JY, Ly JK, Myrick F, Goodman D, White KL, Svarovskaia ES, Borroto-Esoda K, Miller MD. 2009. The triple combination of tenofovir, emtricitabine and efavirenz shows synergistic anti-HIV-1 activity in vitro: a mechanism of action study. Retrovirology 6:44. https://doi.org/10.1186/1742-4690-6-44.
90. Baxter AE, Russell RA, Duncan CJ, Moore MD, Willberg CB, Pablos JL, Finzi A, Kaufmann DE, Ochsenbauer C, Kappes JC, Groot F, Sattentau QJ. 2014. Macrophage infection via selective capture of HIV-1-infected CD4+ T cells. Cell Host Microbe 16:711–721. https://doi.org/10.1016/j.chom.2014.10.010.
91. Real F, Sennepin A, Ganor Y, Schmitt A, Bomsel M. 2018. Live imaging of HIV-1 transfer across T cell virological synapse to epithelial cells that promotes stromal macrophage infection. Cell Rep 23:1794–1805. https://doi.org/10.1016/j.celrep.2018.04.028.
92. Hammonds JE, Beeman N, Ding L, Takushi S, Francis AC, Wang JJ, Melikyan GB, Spearman P. 2017. Siglec-1 initiates formation of the virus-containing compartment and enhances macrophage-to-T cell transmission of HIV-1. PLoS Pathog 13:e1006181. https://doi.org/10.1371/journal.ppat.1006181.
93. Sewald X, Ladinsky MS, Uchil PD, Beloor J, Pi R, Herrmann C, Motamedi N, Murooka TT, Brehm MA, Greiner DL, Shultz LD, Mempel TR, Bjorkman PJ, Kumar P, Mothes W. 2015. Retroviruses use CD169-mediated trans-infection of permissive lymphocytes to establish infection. Science 350:563–567. https://doi.org/10.1126/science.aab2749.
94. Mostoslavsky G, Fabian AJ, Rooney S, Alt FW, Mulligan RC. 2006. Complete correction of murine Artemis immunodeficiency by lentiviral vector-mediated gene transfer. Proc Natl Acad Sci U S A 103:16406–16411. https://doi.org/10.1073/pnas.0608130103.
95. Sixt M, Lammermann T. 2011. In vitro analysis of chemotactic leukocyte migration in 3D environments. Methods Mol Biol 769:149–165. https://doi.org/10.1007/978-1-61779-207-6_11.